

Supporting Information for:

Impact of the Li substructure on the diffusion pathways in alpha and beta Li_3PS_4 : an in-situ high temperature neutron diffraction study

Kavish Kaup,^a Laidong Zhou,^a Ashfia Huq,^b and Linda F. Nazar^{a*}

^a Department of Chemistry, Department of Chemical Engineering and the Waterloo Institute for Nanotechnology, University of Waterloo, 200 University Ave W, Waterloo, Ontario N2L 3G1, Canada

^b Neutron Scattering Division, Oak Ridge National Laboratory, Oak Ridge, Tennessee 37831, United States

Corresponding Author:

*E-mail: lfnazar@uwaterloo.ca

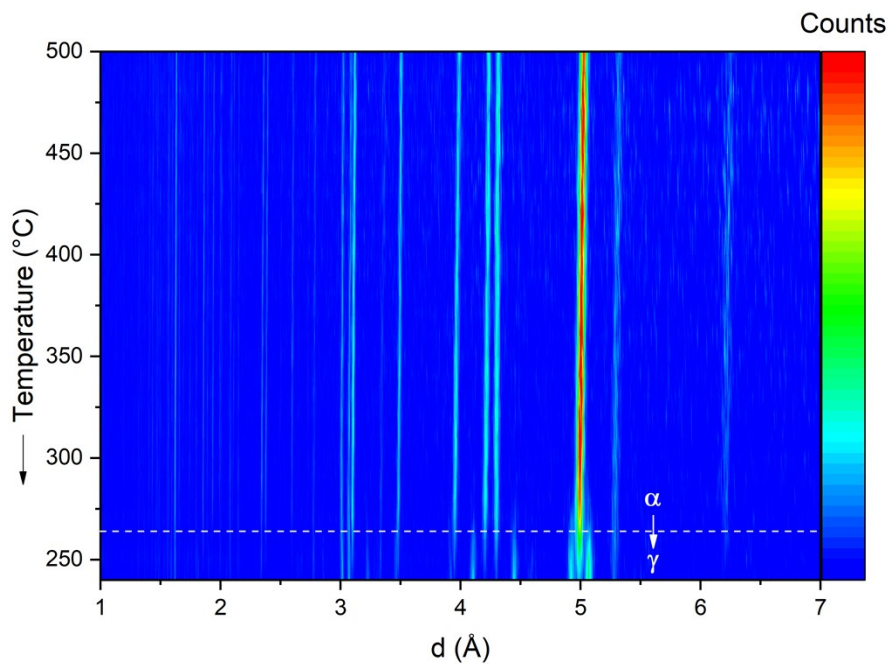


Figure S1: Contour plot upon cooling showing the phase transition from α directly to the γ phase occurs around 260°C.

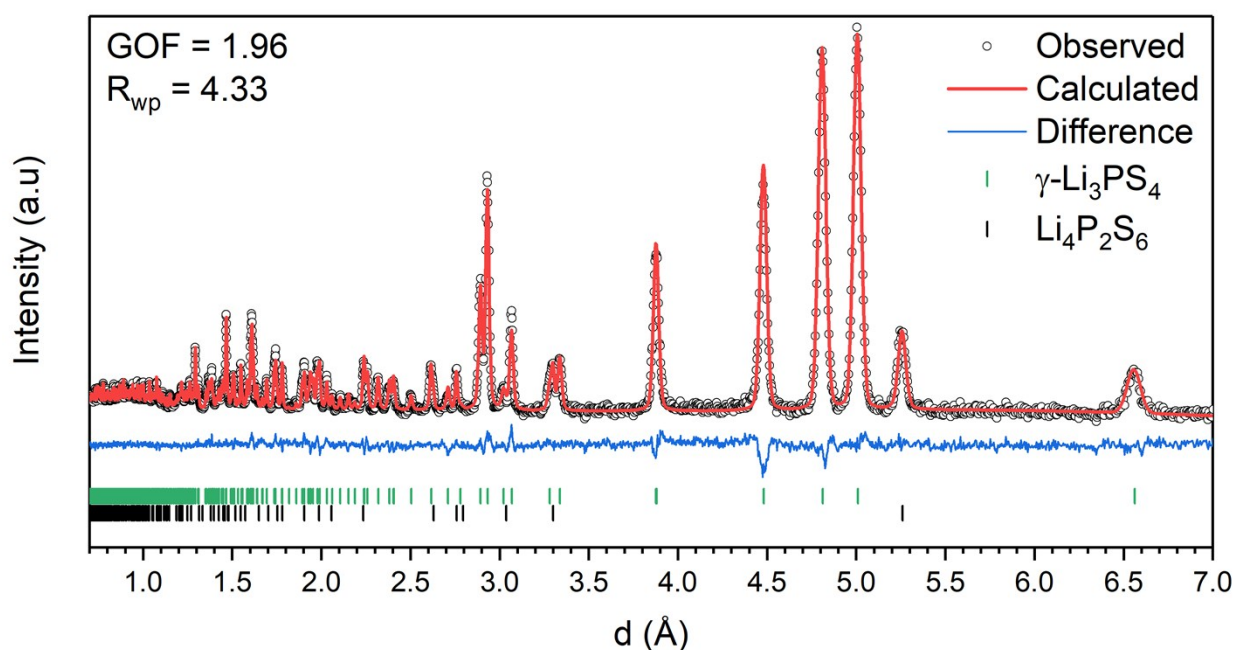


Figure S2: Rietveld refinement of $\gamma\text{-Li}_3\text{PS}_4$ using TOF neutron powder diffraction data measured at 25°C (contains 9 wt.% $\text{Li}_4\text{P}_2\text{S}_6$ impurity).

Table S1: Crystallographic data for $\gamma\text{-Li}_3\text{PS}_4$ obtained from Rietveld refinement of neutron powder diffraction at 25°C. Unit Cell: Orthorhombic $Pmn2_1$ (31). $a = 7.7557(3)$ Å, $b = 6.5627(3)$ Å, $c = 6.1362(3)$ Å, $V = 312.32(2)$ Å³, $Z = 2$

Label	Wyck. Pos.	x	y	z	Occ.	B_{iso} (Å ²)
Li1	4b	0.2441(7)	0.3122(10)	-0.0029(13)	1	1.50(9)
Li2	2a	0	0.1493(15)	0.475(2)	1	2.4(2)
P	2a	0	0.8174(5)	0.9955(4)	1	0.71(5)
S1	4b	0.2177(4)	0.6717(6)	0.8864(6)	1	0.76(7)
S2	2a	0	0.1115(8)	0.8935(9)	1	0.55(10)
S3	2a	0	0.8094(9)	0.3274(6)	1	0.64(11)

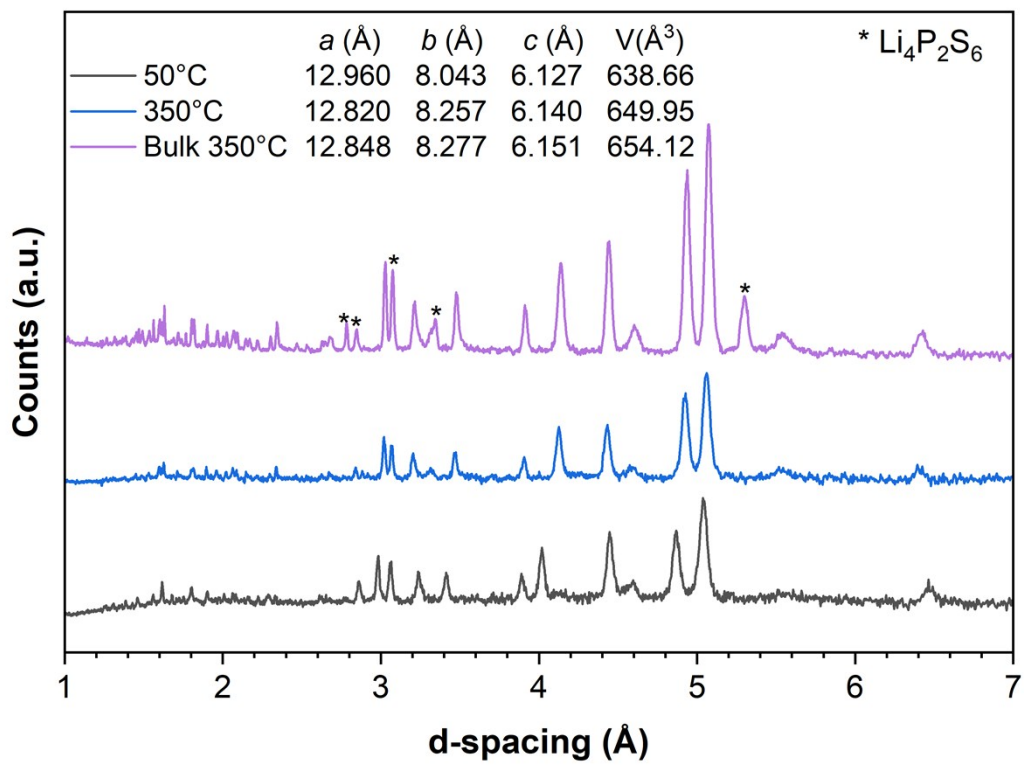


Figure S3: Neutron powder diffraction patterns of nanoporous $\beta\text{-Li}_3\text{PS}_4$ at 50°C and 350°C, compared with bulk $\beta\text{-Li}_3\text{PS}_4$ at 350°C. The lattice parameters were refined from Pawley fits of each diffraction pattern.

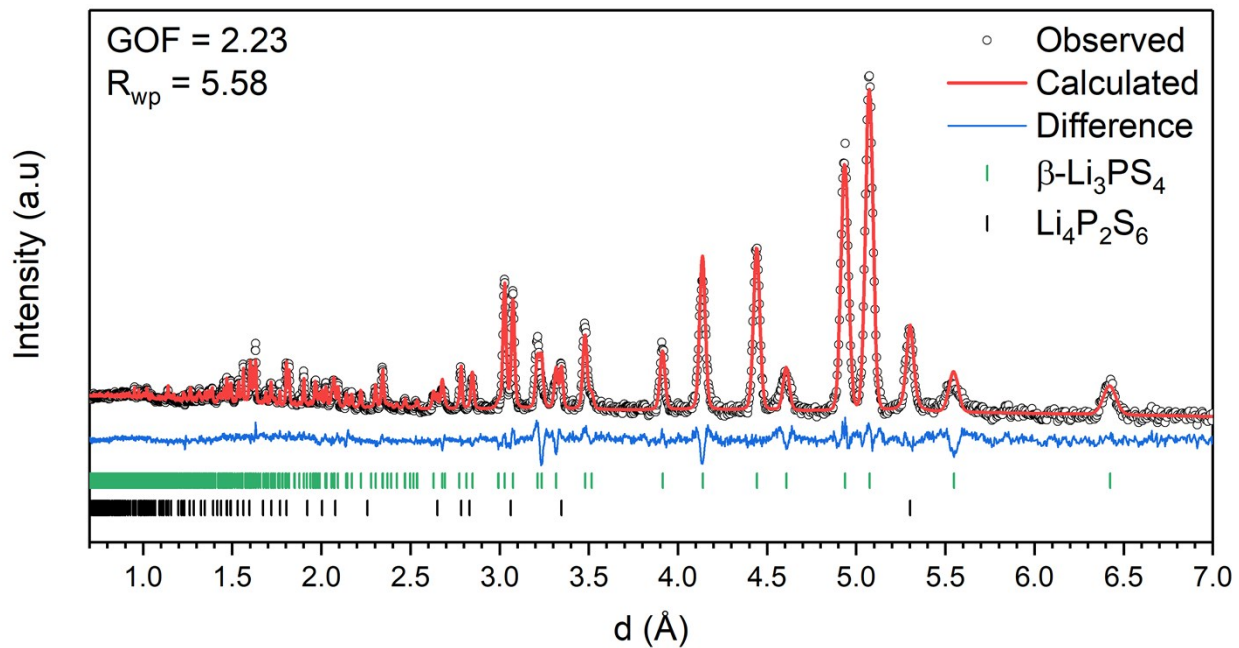


Figure S4: Rietveld refinement of $\beta\text{-Li}_3\text{PS}_4$ using TOF neutron powder diffraction data measured at 350°C (contains 9 wt.% $\text{Li}_4\text{P}_2\text{S}_6$ impurity).

Table S2: Crystallographic data of $\beta\text{-Li}_3\text{PS}_4$ obtained from Rietveld refinement of neutron powder diffraction at 350°C. Unit Cell: Orthorhombic $Pnma$ (62). $a = 12.8483(8)$ \AA , $b = 8.2772(5)$ \AA , $c = 6.1512(3)$ \AA , $V = 654.17(7)$ \AA^3 , $Z = 4$

Label	Wyck. Pos.	x	y	z	Occ.	B_{iso} (\AA^2)
Li1A	8d	0.8489(15)	0.032(2)	0.104(3)	0.666(14)	5.4(4)
Li1B	8d	0.841(3)	0.996(4)	0.371(6)	0.334(14)	5.4(4)
Li2	8d	0.009(3)	0.045(4)	0.582(5)	0.356(8)	5.4(4)
Li3	4c	0.916(5)	$\frac{1}{4}$	0.804(11)	0.288(16)	5.4(4)
P	4c	0.0876(4)	$\frac{1}{4}$	0.1772(10)	1	2.95(14)
S1	8d	0.1548(5)	0.0479(7)	0.2978(13)	1	2.50(11)
S2	4c	0.9360(7)	$\frac{1}{4}$	0.2543(17)	1	2.50(11)
S3	4c	0.1050(7)	$\frac{1}{4}$	0.8461(15)	1	2.50(11)

Table S3: Comparison of the refined structure between nanoporous β -Li₃PS₄ (Stöffler et al.)¹ and bulk β -Li₃PS₄ (this work). Both structures are refined from neutron powder diffraction data

	Nanoporous β -Li ₃ PS ₄ (Stöffler et al.) ¹			Bulk β -Li ₃ PS ₄ (This work)		
Measurement Temperature	25°C			350°C		
Space Group	<i>Pnma</i> (62)			<i>Pnma</i> (62)		
Lattice Parameters (Å)	<i>a</i>	12.993		12.848		
	<i>b</i>	8.0458		8.277		
	<i>c</i>	6.1377		6.151		
Atom	Site	Occ.	(x, y, z)	Site	Occ	(x, y, z)
Li1(A)	8d	1	(0.318, 0.017, 0.139)	8d	0.666	(0.849, 0.032, 0.104)
Li1(B)	-	-	-	8d	0.334	(0.841, 0.996, 0.371)
Li2	4b	0.66	(0, 0, ½)	8d	0.356	(0.009, 0.045, 0.582)
Li3	4c	0.34	(0.442, ¼, 0.55)	4c	0.288	(0.916, ¼, 0.804)
P1	4c	1	(0.088, ¼, 0.167)	4c	1	(0.088, ¼, 0.177)
S1	8d	1	(0.155, 0.0402, 0.267)	8d	1	(0.155, 0.048, 0.298)
S2	4c	1	(0.941, ¼, 0.254)	4c	1	(0.936, ¼, 0.254)
S3	4c	1	(0.101, ¼, 0.801)	4c	1	(0.105, ¼, 0.846)

Table S4: Comparison of the refined structure for α -Li₃PS₄ between the synchrotron powder XRD study by Homma et. al² and the neutron powder diffraction study in this work

	α -Li ₃ PS ₄ (Homma et al.) ²			α -Li ₃ PS ₄ (This work)		
Measurement Temperature	538°C			500°C		
Space Group	<i>Pbcn</i> (60)			<i>Cmcm</i> (63)		
Lattice Parameters (Å)	<i>a</i>	8.603		8.644		
	<i>b</i>	8.997		9.046		
	<i>c</i>	8.439		8.478		
Atom	Site	Occ.	(x, y, z)	Site	Occ	(x, y, z)
Li1	8d	1	(0.738, 0.591, 0.065)	16	0.42	(0.724, 0.353, 0.528)
Li2				8e	0.40	(0.714, 0, 0)
Li3				4c	0.43	(0, 0.196, ¼)
P1	4c	1	(0, 0.827, ¼)	4c	1	(0, 0.831, ¼)
S1	8d	1	(0.307, 0.453, 0.251)	8g	1	(0.304, 0.456, ¼)
S2	8d	1	(0.006, 0.294, 0.549)	8f	1	(0, 0.295, 0.554)

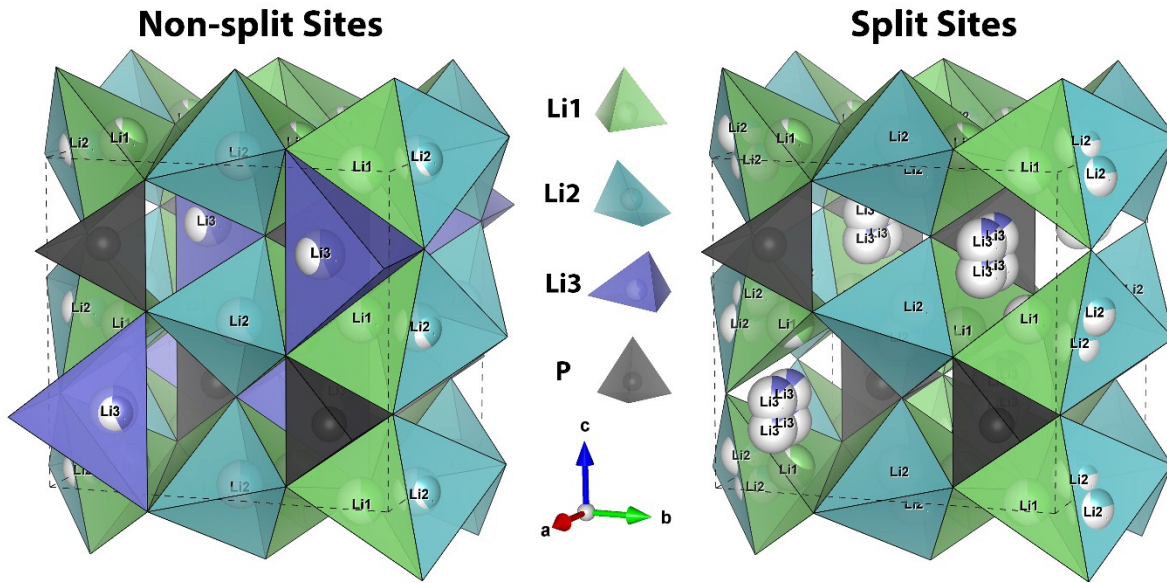


Figure S5: Refined crystal structure of $\alpha\text{-Li}_3\text{PS}_4$ using a model with no site splitting (left) compared to a model with all three lithium sites split (right). Sulfur atoms are omitted for clarity.

Table S5: Bond distances in $\alpha\text{-Li}_3\text{PS}_4$ obtained from Rietveld refinement (using non-split site model) of neutron powder diffraction at 500°C

Center Atom	Second Atom	Interatomic Distance (Å)
Li1	S2	2.45(2) x 2
	S1	2.55(2)
	S1	2.57(2)
Li2	S1	2.293(12) x 2
	S2	2.66(3) x 2
Li3	S2	2.727(16) x 2
	S1	2.75(4) x 2
P	S2	2.015(7) x 2
	S1	2.037(7) x 2
Li1	Li2	1.45(3)
	Li1	1.97(3)
	Li3	2.73(2)

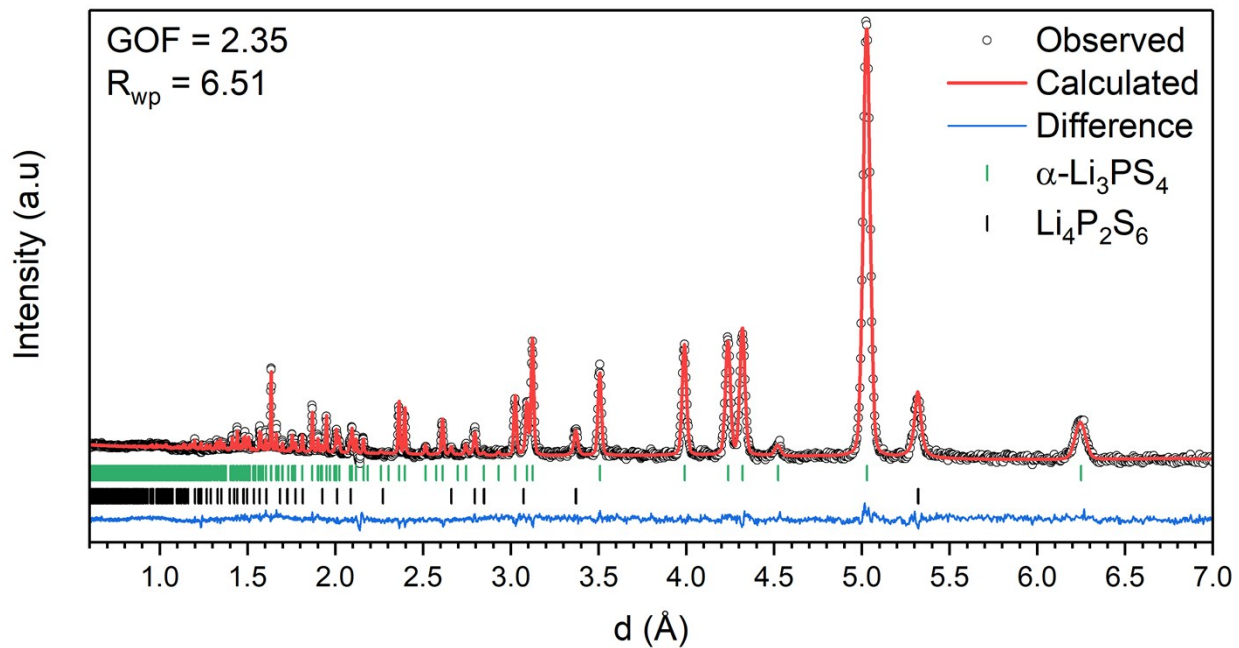


Figure S6: Rietveld refinement of $\alpha\text{-Li}_3\text{PS}_4$ (split-site model) using TOF neutron powder diffraction data measured at 500°C (contains 9 wt.% $\text{Li}_4\text{P}_2\text{S}_6$ impurity).

Table S6: Crystallographic data of $\alpha\text{-Li}_3\text{PS}_4$ (split-site model) obtained from Rietveld refinement of neutron powder diffraction at 500°C. Unit Cell: Orthorhombic Cmcm (63). $a = 8.6437(5)$ Å, $b = 9.0464(5)$ Å, $c = 8.4781(5)$ Å, $V = 662.94(7)$ Å³, $Z = 4$

Label	Wyck. Pos.	x	y	z	Occ.	B _{iso} (Å ²)
Li1	16h	0.724(2)	0.354(2)	0.528(2)	0.400(17)	7.9(8)
Li2	16h	0.716(4)	-0.021(6)	0.047(5)	0.219(11)	7.9(8)
Li3	16h	0.059(4)	0.196(5)	0.207(7)	0.130(15)	7.9(8)
P	4c	0	0.8315(5)	1/4	1	4.04(16)
S1	8g	0.3030(8)	0.4569(7)	1/4	1	5.91(17)
S2	8f	0	0.2944(7)	0.5547(8)	1	5.91(17)

Table S7: Bond distances in α -Li₃PS₄ obtained from Rietveld refinement (using split-sites model) of neutron powder diffraction at 500°C

Center Atom	Second Atom	Interatomic Distance (Å)
Li1	S2	2.45(2)
	S2	2.46(2)
	S1	2.54(2)
	S1	2.56(2)
Li2	S1	1.89(4)
	S2	2.65(5)
	S1	2.69(4)
	S2	2.77(5)
Li3	S2	2.45(6)
	S1	2.49(5)
	S1	3.11(4)
	S2	3.12(6)
P	S2	2.010(7) x 2
	S1	2.046(8) x 2

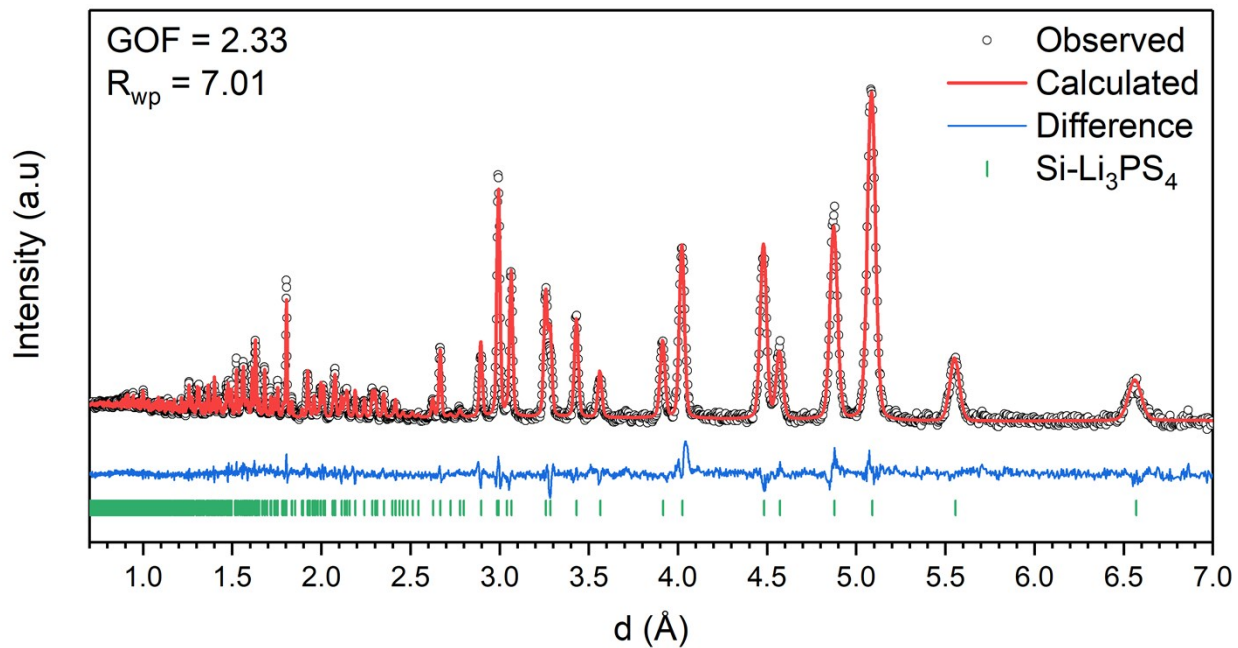


Figure S7: Rietveld refinement of Li_{3.25}Si_{0.25}P_{0.75}S₄ using TOF neutron powder diffraction data measured at 25°C.

Table S8: Crystallographic data of $\text{Li}_{3.25}\text{Si}_{0.25}\text{P}_{0.75}\text{S}_4$ obtained from Rietveld refinement of neutron powder diffraction at 25°C. Unit Cell: Orthorhombic $Pnma$ (62). $a = 13.1420(6)$ Å, $b = 8.0510(3)$ Å, $c = 6.1327(2)$ Å, $V = 648.88(5)$ Å³

Label	Wyck. Pos.	x	y	z	Occ.	B_{iso} (Å ²)
Li1A	8d	0.3330(7)	0.0309(10)	0.3871(15)	0.886(13)	2.96(19)
Li1B	8d	0.360(4)	0.008(8)	0.223(11)	0.114(13)	2.96(19)
Li2	8d	0.0088(12)	0.0400(18)	0.558(2)	0.451(12)	2.1(4)
Li3A	4c	-0.087(5)	¼	-0.159(15)	0.16(2)	2.0(8)
Li3B	4c	-0.080(4)	¼	-0.301(10)	0.20(2)	2.0(8)
P	4c	0.0867(3)	¼	0.1561(5)	0.75	1.58(7)
Si	4c	0.0867(3)	¼	0.1561(5)	0.25	1.58(7)
S1	8d	0.1539(3)	0.0365(5)	0.2753(7)	1	2.02(10)
S2	4c	-0.0620(4)	¼	0.2669(12)	1	1.59(12)
S3	4c	0.1029(4)	¼	-0.1726(9)	1	1.39(11)

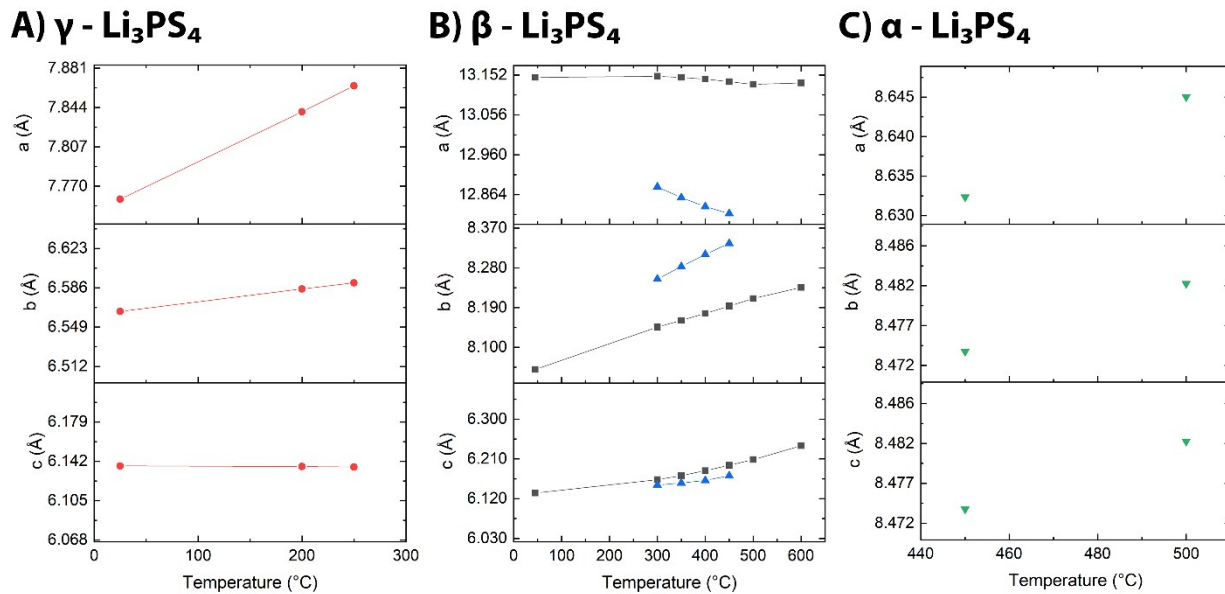


Figure S8: Lattice parameters with increasing temperature of A) bulk γ -LPS (red), B), bulk β -LPS (blue) and β' - $\text{Li}_{3.25}\text{Si}_{0.25}\text{P}_{0.75}\text{S}_4$ (black), and C) bulk α -LPS (green).

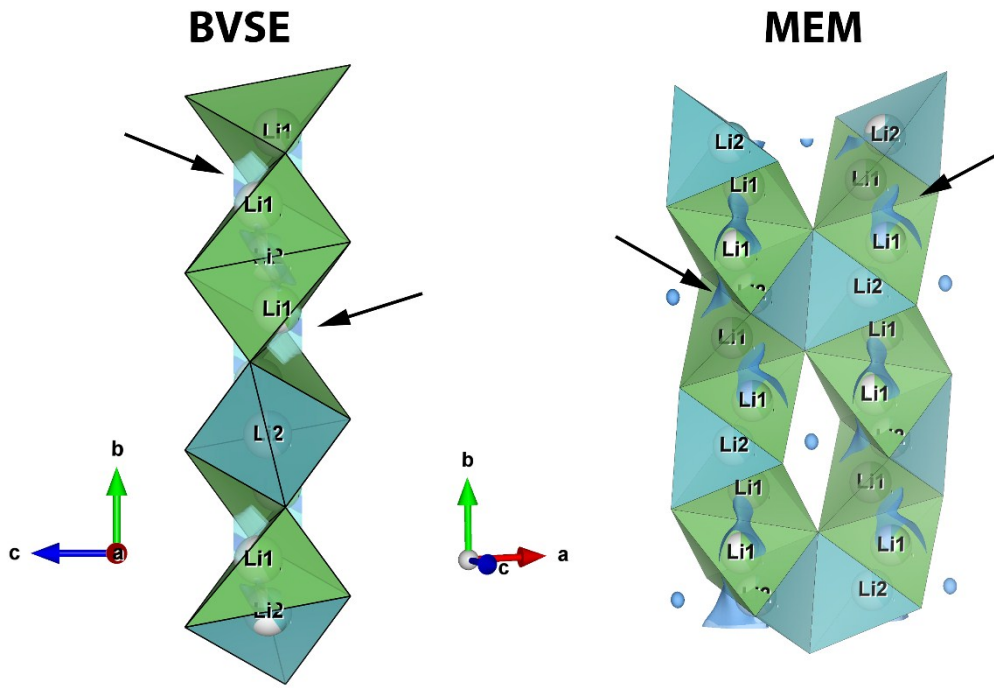


Figure S9: BVSE and MEM map (isosurface of $-0.01 \text{ fm}/\text{\AA}^3$) of $\alpha\text{-Li}_3\text{PS}_4$ showing the linear Li^+ diffusion pathways along the b-axis. Black arrows point to the density from the maps that indicate an interstitial site that connects adjacent $\text{Li}1$ sites.

References

1. H. Stöffler, T. Zinkevich, M. Yavuz, A. Senyshyn, J. Kulisch, P. Hartmann, T. Adermann, S. Randau, F. H. Richter, J. Janek, S. Indris and H. Ehrenberg, *J. Phys. Chem. C*, 2018, **122**, 15954-15965.
2. K. Homma, M. Yonemura, T. Kobayashi, M. Nagao, M. Hirayama and R. Kanno, *Solid State Ionics*, 2011, **182**, 53-58.